University of Tehran

Earth Observation and Geomatics Engineering

Online ISSN: 2588-4360

Homepage: https://eoge.ut.ac.ir/

Assessing Landslide Hazards Along the Haraz Road Based on the NSBAS Processing: Doab Region, April 2022

Zahra Ghorbani[1], **Behzad Voosoghi**[2✉], and **Yasser Maghsoudi**[3]

1. Faculty of Geodesy and Geomatics Engineering, K. N. Toosi University of Technology, Tehran, Iran. E-mail: Zahra.Ghorbani@email.kntu.ac.ir
2. Corresponding author, Faculty of Geodesy and Geomatics Engineering, K. N. Toosi University of Technology, Tehran, Iran. E-mail: vosoghi@kntu.ac.ir
3. Senior Lecturer, Department of Earth and Environmental Sciences, University of Exeter, Penryn, UK. E-mail: y.maghsoudi-mehrani@exeter.ac.uk

Article Info

Article type:
Research Article

Article history:
Received 2024-01-14
Received in revised form 2024-09-29
Accepted 2024-09-30
Available online 2025-01-01

Keywords:
Highway,
Precipitation,
Soil moisture,
Slope instability,
Coherence.

ABSTRACT

Ground movements caused by landslides lead to significant damage and disruption of highway networks in mountainous areas around the world and in Iran, such as the Haraz Road. While difficult to predict, continuous monitoring of land deformation along roads and highways is critical for early identification of hazards before major failures occur. Common slope monitoring approaches using piezometers, inclinometers or geodetic measurements are typically time-consuming and logically challenging. These reactive methods may be effective for smaller locations with movement history but cannot be used for continuous deformation measurement and only apply where sufficient prior movement has occurred to prompt instability signs. Interferometric Synthetic Aperture Radar (InSAR) is a promising option for detecting active landslides over large areas. In this study, we combined Sentinel-1 InSAR (LiCSAR) data products based on the New Small Baseline Subset (NSBAS) processing to estimate ground displacement field from January 2020 to October 2022 in Haraz Road landslide area. Results showed ground deformation ranging from 24-30 mm/year, with most landslides occurring on slopes over 40% grade during the last two years. Time series analysis of ground deformation and rainfall suggests these landslide events tend to occur a few days to a week after heavy rainfall. Coherence change time series also revealed the lowest coherence value of 40, compared to pre-landslide values around 130, in periods following landslide occurrences. Overall, this research demonstrates the value of InSAR and time series analysis for understanding continuous, slow slope movements on roads and unstable areas to help predict possible future landslides.

Cite this article: Ghorbani, Z., Voosoghi, B., & Maghsoudi, Y. (2023). Assessing Landslide Hazards Along the Haraz Road Based on the NSBAS Processing: Doab Region, April 2022. *Earth Observation and Geomatics Engineering*, Volume 7, Issue 2, Pages 1-8. http//doi.org/10.22059/eoge.2024.371085.1145

Publisher: University of Tehran.

DOI: http//doi.org/10.22059/eoge.2024.371085.1145

1. Introduction

Landslides are one of the most destructive and common natural hazards worldwide (Dou et al., 2020). Landslides occur when sloping soil layers are due to external factors such as heavy rainfall, earthquakes and human activities separate and move downwards (Lari et al., 2014). In addition, unstable slopes with slow motion have sufficient potential to damage or weaken engineering infrastructure such as roads, buildings and dams (Cooper et al., 2008; Tomás et al., 2018). Landslides pose a significant threat to road infrastructure in mountainous regions worldwide, including Iran. Recent damaging landslides in Iran have occurred on critical transportation routes such as the Mosulati Givi-Khalkhal road in June 2018, the Haraz Road in April 2022 and or landslides on roads such as Tehran-Chalus in March 2021. These events often result in road closures, traffic delays, and costly emergency repairs. While individual landslides are difficult to predict precisely, continuous monitoring of ground deformation along vulnerable roads can identify emerging hazards before they escalate into major failures.

Traditional deformation monitoring relies on a single point measurement from instruments like inclinometers or GPS/GNSS receivers. While accurate, these techniques are labor-intensive, expensive, and only detect movement at isolated locations on already unstable slopes. Interferometric Synthetic Aperture Radar (InSAR) is one of the promising options as a continuous monitoring tool for ground deformation. It is capable of measuring ground deformations at sub-centimeter scales regardless of weather conditions or day and night. Radar satellites also have short revisiting periods and wide spatial coverage, which enables continuous monitoring of large-scale areas. With the increasing number of satellites and recent advances in InSAR processing techniques, the accuracy of ground deformation measurements keeps improving and is becoming a key technology for detecting geological hazards. By transitioning from reactive point measurements to proactive area monitoring, transportation agencies can better understand landslide hazards, prioritize at-risk locations, and respond more effectively to safeguard road infrastructure against landslide impacts through early warnings, and preventative mitigation measures. Adopting wide-area early warning systems can ultimately reduce landslide costs and impacts while keeping critical transportation links open.

Many studies have used InSAR techniques to assess landslide risk and develop active landslide monitoring mechanisms globally. Examples are provided of studies using Sentinel-1 time series InSAR to analyze landslide behavior and displacement rates in relation to factors like precipitation. For example, Tsironi et al. in 2022 examined the kinematic behavior of active landslides across several sites in the Panachaikon Mountain area, Achaia (Peloponnese, Greece) using Sentinel-1 InSAR time series analysis for the 2016-2021 period. They found that the maximum displacement rate of each landslide was located near its center. Their findings showed that the total precipitation rate can control the increasing displacement rate of an active landslide. Additionally, a vast portion of the Achaia mountainous area suffers from slope instability appearing in various degrees of ground displacement, greatly impacting its morphological features and residential areas (Tsironi et al., 2022). Liu et al. in 2018 utilized a combination of multi-sensor and multi-temporal radar imagery datasets (ALOS/PALSAR 1/2, TerraSAR-X and Sentinel-1A/B) to investigate small-scale loess landslides on the Loess Plateau terrace from December 2006 to November 2017. In total, 32 regions of active landslides were identified from December 2006 to March 2011, and 48 active landslides from January 2016 to November 2016. Moreover, they observed that loess landslides and bedrock landslides exhibit different formation processes (Liu et al., 2018). In another study, Jacquemart and Tiampo (2020) proposed a novel approach for landslide stability assessment using relative interferometric coherence from Sentinel-1 and Normalized Difference Vegetation Index (NDVI) from Sentinel-2. They calculated the ratio of average interferometric coherence or NDVI on an unstable slope to the surrounding hillside slope. They demonstrated that the coherence ratio of the Mad Creek landslide decreased by 50% when the landslide accelerated five months prior to its catastrophic 2017 failure (Jacquemart & Tiampo, 2020).

While past research utilized high-resolution radar data, widespread application of InSAR for large-scale monitoring has been limited by processing costs and data availability. The Sentinel-1 mission provides a unique opportunity for affordable, automated InSAR monitoring over large areas using cloud computing platforms like COMET-LiCSAR (Lazecký et al., 2020; Wright et al., 2023; Sadeghi et al., 2023; Ghorbani et al., 2023; Babaei et al., 2024; Ghorbani et al., 2024). This research proposes processing LiCSAR products and applying atmospheric correction to reduce noise. The aim is to improve the automatic identification of signs of slope instability along Haraz Road. Time series InSAR deformation and coherence data will be evaluated alongside instability triggers like rainfall and soil moisture levels. The results will promote further understanding of gradual, ongoing slope movements in unstable areas and enable early warning of potential landslides affecting vital Haraz Road infrastructure.

2. Description of study area and data

The Haraz Road axis is a critical transportation route in Iran's Mazandaran province. This area features diverse geology that heightens the risk of hazards directly impacting transportation infrastructure (Figure 1). Careful attention to geological characteristics is vital when constructing, maintaining, or repairing systems along this route. Limestone, marl, sandstone, shale, and river sediments comprise most roadside outcrops. Igneous and pyroclastic rocks also emerge, often related to Eocene and Jurassic volcanic deposits. The discontinuities between sedimentary

strata and volcanic intrusions can exacerbate slippage and collapse hazards despite the abundance of fractures and joints (Dehghan Farouji & Beitollahi, 2022). The Razan landslide zone in the Central Alborz Mountains poses a significant risk for the region. This area was originally an ancient landslide thought to have been triggered by a major earthquake along the North Alborz fault in past millennia. More recently, the zone has become destabilized due to extensive mining of sand and gravel for construction materials. Given the freshly disturbed geology and continuing mining extractions, the Razan landslide zone remains highly prone to future slides. This represents a concern for the nearby Haraz Road which traverses the zone. Mitigation of landslide risk in the Razan area will require restrictions on mining activities and stabilization of the most vulnerable slopes overlooking the highway.

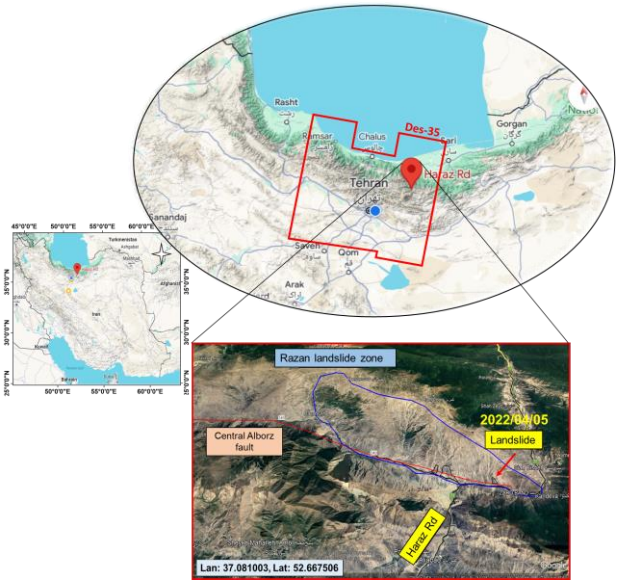

Figure 1. Geographical location of the Razan landslide zone and the frame of Sentinel-1 InSAR (LiCSAR) images that covers the Haraz Road area.

Given the necessity of understanding landslide hazards for transportation networks, this study performs time series analyses of landslide detection using Sentinel-1 radar data. We acquired 80 Sentinel-1 images spanning January 2020 to October 2022 over a 250 km 2 area of the Haraz Road axis. The 12-day interval dataset from the satellites' descending orbit enabled interferometric processing and derivation of unwrapping phase and coherence products (Figure 2). These are obtained from the COMET-LiCS portal (*https://comet.nerc.ac.uk/COMET-LiCS-portal/*) to detect and characterize landslide risks along this critical Iranian highway over time.

3. NSBAS processing by LiCSBAS time-series analysis

LiCSBAS is an open-source package based on Python coding to carry out InSAR time series analysis using LiCSAR products (i.e. unwrapped interferograms and coherence, GACOS data) that are freely available on the COMET-LiCS web portal (Morishita et al., 2020). Initially, we downloaded LiCSAR products automatically by running the script. Then the conversion file format was done. In the next step, to reduce the impact of unwrapping errors in Haraz region, before the subsequent time-series analysis, pixels with a coherence of 0.1 are masked and then the data are unwrapped automatically using SNAPHU (Hanssen, 2001). Thereafter, all the unwrapped data and corresponding coherence images are clipped to the Haraz region. The unwrapped coverage and coherence threshold are set to <0.5 and 0.06, respectively. The unwrapped interferograms are resampled and geocoded using the Shuttle Radar Topography Mission Digital Elevation Model (SRTM DEM 30 m). Overall, the baseline network obtained from Sentinel-1 images for the descending (D-35) tracks include 388 interferogram that contain noisy data or do not pass a phase loop closure test (indicating severe unwrapping errors) are automatically excluded from the analysis. To estimate the ground displacement field and velocity of a surface pixel over time using a sequence of displacement data, a Small Baseline inversion is carried out on the network of interferograms. If we possess a stack containing M-unwrapped interferograms:

$$d = \left[d_1, ..., d_M \right]^T \quad (1)$$

Produced from N images taken at ordered times ($t0,\ldots,N\text{-}1$), N-1 incremental displacement vector and

$$m = \left[m_1, ..., m_{N-1} \right]^T \quad (2)$$

(i.e., m_i is the incremental displacement between time t_{i-1} and t_i) can be derived by solving:

$$d = Gm \quad (3)$$
$$G = M \times (N-1) \quad (4)$$

where G is a design matrix of zeros and ones describing the relationship between the network of the considering that the unwrapped interferogram is the sum of corresponding successive incremental displacements (Morishita et al., 2020). Cumulative displacements for each acquisition (i.e., the displacement time series) are simply calculated by summing the incremental displacements. The mean displacement velocity is then derived from the cumulative displacements by least-squares. Even though Sentinel-1 data are constantly being acquired with short spatial and temporal baselines in most areas, there could still be gaps in the Small Baseline network due to decorrelation associated (Morishita et al., 2020).

The New Small Baseline Subset (NSBAS) approach proposed by López-Quiroz et al. (2009) and Doin et al.

(2011) is used to obtain more realistic displacement time series even with a disconnected satellite image network. Thus, NSBAS can estimate displacements across network gaps by assuming linear motion by Equation (5). Then, the constrained system can be solved by a least-square inversion in Equation (6). This allows NSBAS processing by LiCSBAS time-series analysis to provide velocity estimates over larger areas, particularly in low coherence regions, compared to the traditional Small Baseline Subset (SBAS) implementation which skips all processing for any column containing a NaN (Maghsoudi et al., 2022; Ghorbani et al., 2022).

$$d = vt + c \tag{5}$$

$$\begin{bmatrix} \boldsymbol{d}_1 \\ \vdots \\ \boldsymbol{d}_M \\ 0 \\ \vdots \\ 0 \end{bmatrix} = \begin{bmatrix} \begin{bmatrix} & \boldsymbol{G} & \end{bmatrix} \begin{bmatrix} 0 & 0 \\ \vdots & \vdots \\ 0 & 0 \end{bmatrix} \\ \gamma \begin{bmatrix} 1 & 0 & \dots & \dots & 0 & -t_1 & -1 \\ \vdots & \ddots & \ddots & & \vdots & -t_2 & \vdots \\ 1 & \dots & 1 & \ddots & \vdots & \vdots & \vdots \\ \vdots & & \vdots & \ddots & 0 & \vdots & \vdots \\ 1 & \dots & 1 & \dots & 1 & -t_{N-1} & -1 \end{bmatrix} \end{bmatrix} \begin{bmatrix} \boldsymbol{m}_1 \\ \vdots \\ \boldsymbol{m}_M \\ v \\ c \end{bmatrix} \tag{6}$$

where γ is a scaling (weighting) factor of the temporal constraint.

Centre for Medium-Range Weather Forecasts (ECMWF) data based Generic Atmospheric Correction Online Service for InSAR (GACOS) were utilized to correction of the tropospheric noise present in interferograms (*http://www.gacos.net/*). According to Figure 3(a,b), the standard deviation (STD) of unwrapped phases before and after GACOS corrections has been calculated to reduce tropospheric noise for each interferogram. GACOS corrections significantly reduced the STD for each interferogram from an average of 2.8 rad to 2.5 rad overall Figure 3(c). For some interferometers, the phase noise was reduced by 50% on average, from 2.7 rad down to 1.2 rad. Finally, after GACOS corrections, the maps are high-pass filtered in time and low-pass filtered in space, to separate noise components from the displacement time series.

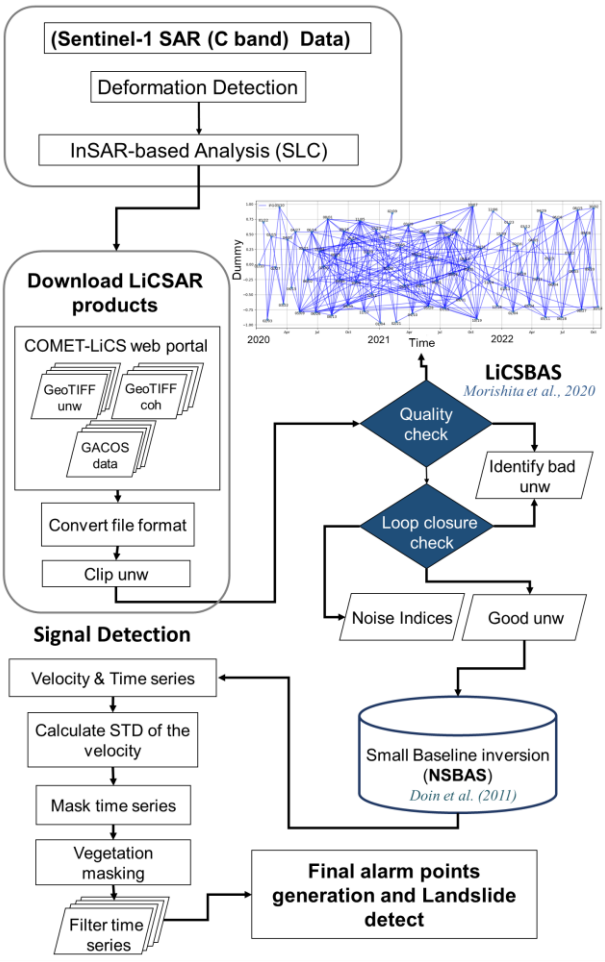

Figure 2. The process of analysing InSAR data to measure the ground displacement field.

4. Results

We estimated the surface deformation time series at each landslide location in the Haraz Road using LiCSBAS. Then, assessed the relationship between InSAR time series with precipitation and soil moisture.

4.1. Ground deformation derived by LiCSBAS

The ground deformation map along with the slope map for further interpretation of the Haraz Road area is shown in Figure 4. Figure 4a shows the map of the mean displacement velocity in the sensor line of sight (LOS) from January 2020 to October 2022 in the Haraz Road area. The mean displacement velocity is estimated between -24 mm/yr to +14 mm/yr during the 2-year observation period. The red colors in the deformation map indicate moving away from the satellite (subsidence), while blue colors indicate uplift and moving towards the satellite. Subsidence is mostly observed in places with gentle to steep slopes (<5%) (Figure 4b).

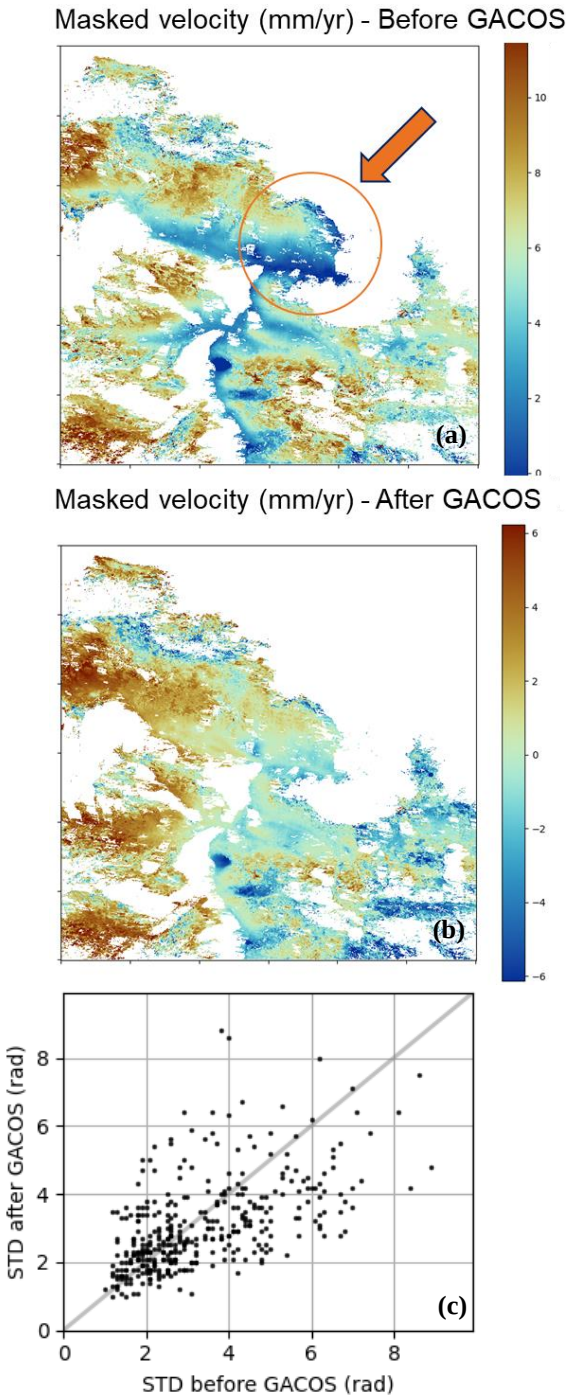

Figure 3. Effect of tropospheric phase delay correction of each interferogram using GACOS based on weather forecast model (ECMWF) at (a) before GACOS, (b) after GACOS and (c) correlation diagram of the STD of unwrapped phases before and after the GACOS correction.

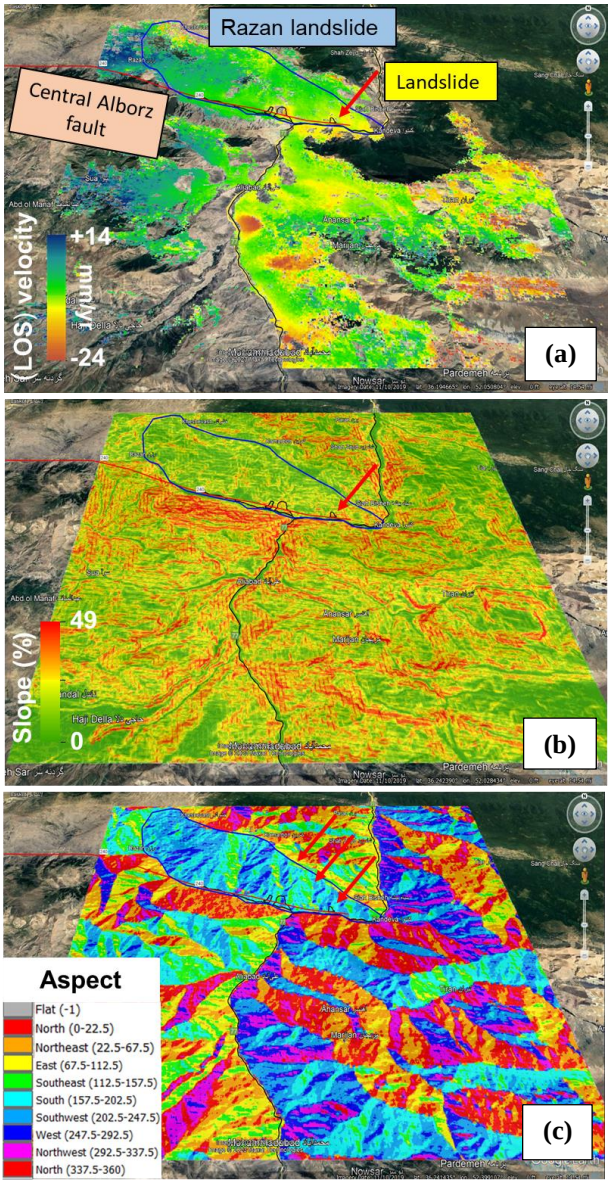

Figure 4. The ground deformation map along with (a) the mean LOS velocity map obtained from LiCSAR data products by LiCSBAS from, (b) Slope map and (c) Aspect.

As a result, the main subsidence found (from -24 mm/yr to -10 mm/yr) is observed in the southeastern and southern areas around the road. Positive displacement values are also seen in most areas with a very gentle slope in the study area, especially in flat areas such as the upstream areas of the road. The green areas in the map indicate the sensitivity of low risk areas where landslides are unlikely to occur but may sometimes occur. The yellow to red colors in the steep slope indicate areas where the probability of landslide and soil erosion is higher. As can be seen in the figure, most deformation pixels located in areas with slopes above 40% were more at risk of collapse. In fact, it can be concluded that active landslides are moving in the same direction as the

deformed pixels towards the south and southwest along the road (Figure 4c). Our research results show that the most deformation of active landslide masses has occurred along the Haraz-Baladeh Road in the Razan landslide zone. Those located at the lowest part of the mountains near the road have recorded the highest mean velocity of deformation along the sensor line-of-sight for monitoring (generally between -6 mm/yr and +5 mm/yr) and well delineate the landslide boundary (Figure 5). Three identified active landslide locations in this landslide zone include the debris slide occurred in the afternoon of 2 April 2022 (A), the mining (B) and the mountain thrust due to explosion and mining in the summer of 2021 (C), having the highest deformation potential indicating a relatively steep slope.

For further interpretation, the annual deformation time-series of the region were carried out using LiCSBAS. This allows us to determine whether the unstable slope conditions pre-existed or are still ongoing. Figure 6 shows the deformation time-series at the three landslide locations from January 2020 to October 2022. The results indicate that the reported time frame of the mountain thrust landslide activity along the Haraz Road, the period of April 5, 2022, with a deformation rate of about 8 mm/yr had the highest deformation potential. Landslides in Noor valley in the Central Alborz occurred along major faults such as the Baladeh fault and on the important North Alborz fault hanging wall. Therefore, this region along the Haraz Road is at risk in terms of landslides during rainfall and earthquakes and other hazards, and attention to construction and the existence of an early warning system is essential disaster management in these areas.

By observing the LiCSBAS InSAR time-series, rainfall and reviewing the soil moisture data in the area in Figure 7, it becomes clear that the landslide deformation is closely related to precipitation. With increasing intensity and duration of rainfall, water infiltration into the soil increases. This situation has affected the increase in weight and pores. When water continuously enters impermeable soil that acts as a viscous surface, the ground becomes unstable and weathering causes ground movement. The change in water content in the soil causes a difference in soil properties, reducing soil resistance (Blasio et al., 2011; Serrano et al., 2019). To assess the impact of precipitation in this area, satellite precipitation data from the Global Precipitation Measurement (GPM) mission were used (https://gpm.nasa.gov/missions/GPM) (Figure 7a). The average annual precipitation in the study area is about 17 mm and the highest amount of precipitation belongs to the months of April. Also, the soil moisture at shallow and subsurface depths of the soil layer has been calculated based on the satellite dataset Soil Moisture Active Passive (SMAP) (*https://smap.jpl.nasa.gov/*).

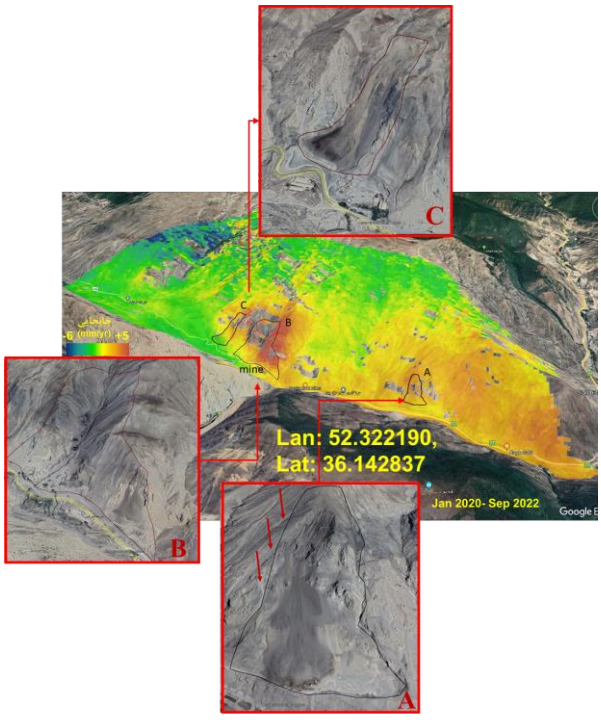

Figure 5. Mean LOS velocity map derived from LiCSAR data products by LiCSBAS at three landslide locations (A, B and C). The red color zones indicate a higher potential for landslide activity.

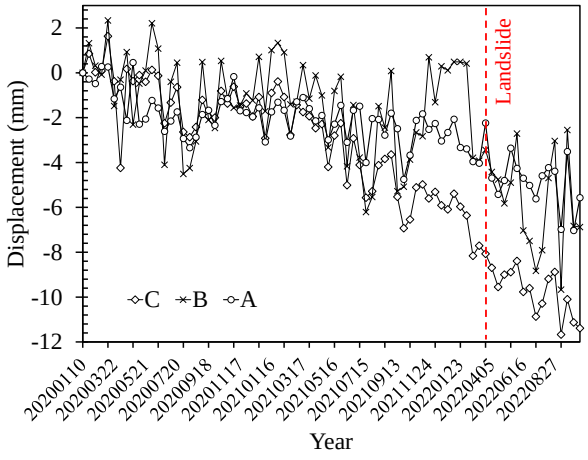

Figure 6. Time-series of deformation from LiCSAR data products at three landslide locations (A, B and C).

4.2. Assessing of LiCSBAS time series with precipitation and soil moisture data

It is observed that the highest amount of soil moisture from November 2021 to April 2022 is estimated at 100 mm. Therefore, we detect deformation before the catastrophic collapse of a large slope on Haraz Road, which has dramatically changed the natural landscape due to the landslide. The landslide occurred on April 5, 2022, after the first spring rains. Given the available reports on the mountain slip on the Haraz Road, mining operations

continued until mid-March 2022, but due to the Nowruz holidays, there were no mining-related explosions. It can be understood that the implementation of sand and gravel quarrying operations from the landslide toe of Razan has affected the occurrence of the landslide, but the main reason according to the time series is recent rainfall and increased soil moisture before the landslide. This landslide at kilometer 44 of Haraz Road caused a debris flow that trapped people in dust and they could not pass through this area. The time series of deformations obtained from radar observations at location A show that before the landslide, there was no significant displacement until the time interval of February 16, 2022, and the slope around the road was stable. But from the time interval of February 28, 2022, to April 5, 2022, due to the instability of the slope and slow movements of the ground surface up to the debris flow, the displacement rate of sliding areas reaches 8 millimeters per year. The downward trend in displacement rate from April 5, 2022, has been slowly changing in slopes around the area. Also, given the daily precipitation of the area, it is observed that approximately 10 days before the landslide and cessation of rainfall, the increase in precipitation was about 8 millimeters. As a result, we recognize that these events may have been located a few days or a week before.

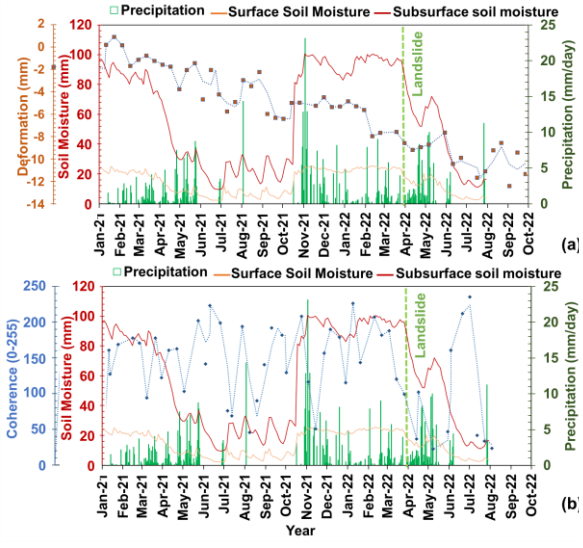

Figure 7. Evaluation of InSAR deformation time-series and radar coherence at the mountain landslide site (A) from January 2021 to October 2022 with (a) daily precipitation time-series by GPM mission data and (b) soil moisture time-series from SMAP data.

To examine the distinction between coherence loss due to the landslide under investigation and natural coherence loss, we used a time series of radar coherence derived from interferometric pairs with similar acquisition dates before and after the slope instability and mountain slide. The average value of coherence changes in the time interval of the landslide occurrence (with the amount of 90) compared to before and after the landslide event is 130 and 40, respectively, in the displacement range of location A.

5. Conclusion

Given the history of landslides and other geotechnical disruptions on Haraz Road in recent years, continuous monitoring and study of this phenomenon is crucial for effective control and management. This study successfully applied InSAR time series analysis to examine deformation at multiple landslide locations, identifying different characteristics of landslides in the region. By combining LiCSAR data products with the LiCSBAS processing package, we obtained detailed surface deformation rates at each landslide location. Our results revealed a mean deformation velocity of 24 mm/yr during the period from January 2020 to October 2022. The most significant deformation occurred in the rockfall deposition zone and the large sliding zone of Razan. Notably, landslide locations with slopes less than 40% showed the highest potential for deformation, indicating relatively steep terrain. The direction of deformed pixels was predominantly towards the south and southwest. The study demonstrated a clear relationship between landslide deformation, precipitation, and soil moisture. A significant landslide event on April 5, 2022, with a deformation rate of about 8 mm/yr, coincided with heavy rainfall. Analysis of hourly precipitation data showed an increase of about 10 mm approximately 10 days before the landslide occurred, suggesting a potential window for early warning. Importantly, the time series of changes in mean coherence values provided additional insights. The lowest coherence value of 40 corresponded to the period of landslide occurrence, indicating a potential indicator for detecting major ground movements. This research not only contributes to the understanding of landslide dynamics along the Haraz Road but also demonstrates the effectiveness of InSAR time series analysis for landslide monitoring and early warning. The method developed in this study shows promise for detecting and providing early warnings for major landslides, which could significantly improve road safety and infrastructure management in landslide-prone areas. Future work could benefit from integrating ground-based measurements, conducting sensitivity analyses of NSBAS processing parameters, and incorporating additional environmental variables such as vegetation cover, longitudinal slope profiles and machine learning. These enhancements would further refine the methodology and potentially improve the accuracy of landslide prediction and risk assessment.

References

Dou J, Yunus AP, Bui DT, Merghadi A, Sahana M, Zhu Z, Chen C-W, Han Z, Pham BT. 2020. Improved landslide assessment using support vector machine with bagging, boosting, and stacking ensemble machine learning framework in a mountainous watershed, Japan. Landslides. 17(3):641–658. *http://dx.doi.org/10.1007/s10346-019-01286-5.*

Lari S, Frattini P, Crosta GB. A probabilistic approach for landslide hazard analysis. Engineering Geology. 2014;182:3-14. *https://doi.org/10.1016/j.enggeo.2014.07.015*.

Cooper, A.H. The classification, recording, databasing and use of information about building damage caused by subsidence and landslides. Q. J. Eng. Geol. Hydrogeol. 2008, 41, 409–424, *https://doi.org/10.1144/1470-9236/07-223*.

Tomás, R.; Abellán, A.; Cano, M.; Riquelme, A.; Tenza-Abril, A.J.; Baeza-Brotons, F.; Saval, J.M.; Jaboyedoff, M. A multidisciplinary approach for the investigation of a rock spreading on an urban slope. Landslides 2018, 15, 199–217, *https://www.annalsofgeophysics.eu/index.php/annals/article/view/8633*.

Tsironi, V., Ganas, A., Karamitros, I., Efstathiou, E., Koukouvelas, I., & Sokos, E. Kinematics of Active Landslides in Achaia (Peloponnese, Greece) through InSAR Time Series Analysis and Relation to Rainfall Patterns. Remote Sensing, 14(4), 844 (2022), *https://doi.org/10.3390/rs14040844*.

Liu, X., Zhao, C., Zhang, Q., Peng, J., Zhu, W., & Lu, Z. Multi-temporal loess landslide inventory mapping with C-, X-and L-band SAR datasets—A case study of Heifangtai Loess Landslides, China. Remote sensing, 10(11), 1756 (2018), *https://doi.org/10.3390/rs10111756*.

Jacquemart, M., & Tiampo, K. Radar coherence and NDVI ratios as landslide early warning indicators. Natural Hazards and Earth System Sciences Discussions, 1-16 (2020), *https://doi.org/10.5194/nhess-2020-227*.

Lazecký, M.; Spaans, K.; González, P.J.; Maghsoudi, Y.; Morishita, Y.; Albino, F.; Elliott, J.; Greenall, N.; Hatton, E.; Hooper, A.; Juncu, D.; McDougall, A.; Walters, R.J.; Watson, C.S.; Weiss, J.R.; Wright, T.J. LiCSAR: An Automatic InSAR Tool for Measuring and Monitoring Tectonic and Volcanic Activity. Remote Sensing, 2020, 12, 2430. *https://doi.org/10.3390/rs12152430*.

Ghorbani, Z., Darzi, A. G., Sadeghi, H., & Garakani, A. A. (2023). Field reconnaissance and InSAR investigation of subsidence-induced damage to electricity dispatch centers–A case study in Tehran. In Smart Geotechnics for Smart Societies (pp. 1200-1203). CRC Press, *https://doi.org/10.1201/9781003299127-171*.

Sadeghi, H., Darzi, A. G., Voosoghi, B., Garakani, A. A., Ghorbani, Z., & Mojtahedi, S. F. F. Assessing the vulnerability of Iran to subsidence hazard using a hierarchical FUCOM-GIS framework. Remote Sensing Applications: Society and Environment, 31, 100989 (2023). *https://doi.org/10.1016/j.rsase.2023.100989*.

Ghorbani, Z., Khosravi, A., Maghsoudi, Y., Mojtahedi, F. F., Javadnia, E., & Nazari, A. (2022). Use of InSAR data for measuring land subsidence induced by groundwater withdrawal and climate change in Ardabil Plain, Iran. Scientific Reports, 12(1), 13998, *https://doi.org/10.1038/s41598-022-17438-y*.

Dehghan Farouji, F., & Beitollahi, A. (2022). The geology of the Haraz road in the province of Mazandaran with emphasis on Identifying natural hazards. Road, 30(113), 33-56, *https://doi.org/10.22034/road.2022.77104*.

Morishita, Y., Lazecky, M., Wright, T. J., Weiss, J. R., Elliott, J. R., & Hooper, A. LiCSBAS: An open-source InSAR time series analysis package integrated with the LiCSAR automated Sentinel-1 InSAR processor. Remote Sensing, 12(3), 424 (2020). *https://doi.org/10.3390/rs12030424*.

Hanssen, R.F. Radar Interferometry: Remote Sensing and Digital Image Processing; Springer: Dordrecht, The Netherlands, 2001; Volume 2, ISBN 978-0-7923-6945-5, *http://dx.doi.org/10.1007/0-306-47633-9*.

Doin, M.-P.; Lodge, F.; Guillaso, S.; Jolivet, R.; Lasserre, C.; Ducret, G.; Grandin, R.; Pathier, E.; Pinel, V. Presentation of the small baseline NSBAS processing chain on a case example: The Etna deformation monitoring from 2003 to 2010 using Envisat data. In Proceedings of the Fringe 2011 Workshop, Frascati, Italy, 19–23 September 2011, *https://ens.hal.science/hal-02185213v1*.

López-Quiroz, P., Doin, M. P., Tupin, F., Briole, P., & Nicolas, J. M. (2009). Time series analysis of Mexico City subsidence constrained by radar interferometry. Journal of Applied Geophysics, 69(1), *1-15, https://doi.org/10.1016/j.jappgeo.2009.02.006*.

Blasio, F. V. Introduction to the physics of landslides. New York: Springer (2011). *https://doi.org/10.1007/978-94-007-1122-8*.

Serrano, J., Shahidian, S., & Marques da Silva, J. Evaluation of normalized difference water index as a tool for monitoring pasture seasonal and inter-annual variability in a Mediterranean agro-silvo-pastoral system. Water, 11(1), 62 (2019), *https://doi.org/10.3390/w11010062*.

Maghsoudi, Y., Hooper, A. J., Wright, T. J., Lazecky, M., & Ansari, H. (2022). Characterizing and correcting phase biases in short-term, multilooked interferograms. Remote Sensing of Environment, 275, 113022, *https://doi.org/10.1016/j.rse.2022.113022*.

Wright, T. J., Houseman, G., Fang, J., Maghsoudi, Y., Hooper, A., Elliott, J., ... & Wang, H. (2023). High-resolution geodetic strain rate field reveals dynamics of the India-Eurasia collision, *https://doi.org/10.31223/X5G95R*.

Ghorbani, Z., Khosravi, A., Maghsoudi, Y., & Voosoghi, B. (2024). InSAR Measurements for Landslide-Induced Damage Assessment on Part of North Alabama Highway, Morgan County. In Geo-Congress 2024 (pp. 523-532), *http://dx.doi.org/10.1061/9780784485347.053*.

Babaei, A., Sadeghi, H., & Ghorbani, Z. (2024). Deep Neural Networks for Predicting the Settlement of Earth Dams Based on the InSAR Outputs. Indonesian Geotechnical Journal, 3(2), 57-66, *https://doi.org/10.56144/igj.v3i2.102*.